Spatially Controlled Reduction and Growth of Silver in Hollow Gold Nanoshell Particles

Lu Zhang, Peng Chen, Alexis Loiseau, Dalil Brouri, Sandra Casale, Michèle Salmain, Souhir Boujday, Bo Liedberg

Spatially controlled reduction and growth of silver in hollow gold nanoshell particles

Zhang, Lu; Chen, Peng; Loiseau, Alexis; Brouri, Dalil; Casale, Sandra; Salmain, Michèle; Boujday, Souhir; Liedberg, Bo

2019

Zhang, L., Chen, P., Loiseau, A., Brouri, D., Casale, S., Salmain, M., ... Liedberg, B. (2019). Spatially controlled reduction and growth of silver in hollow gold nanoshell particles. The Journal of Physical Chemistry C, 123(16), 10614-10621. doi:10.1021/acs.jpcc.8b11864

https://hdl.handle.net/10356/143199

https://doi.org/10.1021/acs.jpcc.8b11864

Spatially Controlled Reduction and Growth of Silver in Hollow Gold Nanoshell Particles

Lu Zhang[1,2,3‡,] Peng Chen[1‡,] Alexis Loiseau[2], Dalil Brouri[2], Sandra Casale[2], Michèle Salmain[4,5], Souhir Boujday*[2,5], Bo Liedberg*[1,5]

[1]*Centre for Biomimetic Sensor Science, School of Materials Science and Engineering, Nanyang Technological University, Singapore 637553.*

[2]*Sorbonne Université, CNRS, Laboratoire de Réactivité de Surface (LRS), 4 place Jussieu, F-75005 Paris, France.*

[3]*Sorbonne University-Nanyang Technological University Dual Degree PhD Programme.*

[4]*Sorbonne Université, CNRS, Institut Parisien de Chimie Moléculaire (IPCM), 4 place Jussieu F-75005 Paris, France.*

5*Majulab, International Joint Research Unit UMI 3654, CNRS, Université Côte d'Azur, Sorbonne Université, National University of Singapore, Nanyang Technological University, Singapore.*

ABSTRACT: Spatially controlled reactions at the nanoscale have attracted increasing interest for fundamental chemistry and for the engineering of novel functional materials. Herein, we demonstrate that pH-triggered reduction of silver ions preferentially occurs at the inner walls of porous and citrate capped gold nanoshell (AuNS) particles. The reaction initially relies on the presence of sacrificial silver ions inside the AuNS particles as well as in the surrounding preparation solution, and it proceeds upon external addition of silver ions until a solid silver core is formed inside the AuNS particles. Subsequent reduction of silver occurs on the external surface of the solidified AuNS resulting in a layered and compositionally complex nanoparticle containing both silver and gold. Growth experiments performed in the dark, under white light illumination as well as near resonance suggest that the reduction reaction is not guided by a plasmonic field enhancement effect. This is in contrast to the recently proposed hot spot mechanism of silver reduction at the rim of nanoholes in a periodic gold array. Our observations point towards a confinement process that proceeds *via* a continuous supply of silver ions that diffuses from the external solution through the porous shell into the inner volume of the AuNS particles where they become reduced.

INTRODUCTION

Spatially controlled chemical reactions have attracted much attention both in fundamental research and applications.[1-3] More importantly, if the reaction can be precisely controlled at the nanoscale, it may even lead to a revolution in both traditional chemistry and nanotechnology.[4-6] For example, Localized Surface Plasmon Resonance (LSPR) is a phenomenon where surface electrons are brought in resonance with an external electromagnetic field and it offers opportunities to confine the light to a regime below diffraction limit. Plasmonic materials thus can be used as nanoscale light sources to selectively boost chemical reactions at the nanoscale, which is known as "plasmonic nanochemistry". Pioneering works have been done on spatially controlled chemical reactions by controlling the local plasmonic fields/hot spots of metal nanoparticles/structures.[6-9] Among those, Ai *et al.* studied the plasmonic guided chemical reduction of Ag^+ in gold nanohole array using TEM imaging.[6] They found that the sites of Ag growth perfectly matched the hotspots on the gold nanohole array predicted by finite-difference time-domain (FDTD) simulations.

In contrast to the aforementioned plasmonic strategy, nanoconfinement also has been explored to physically control chemical reactions inside nanosized reactors.[10,11] Interestingly, in a nanosized space the chemistry, reaction paths, equilibrium, activities and dynamics etc. can be very different from that of bulk.[11-17] Different materials have been explored as reactors for nanoconfined chemical reactions, including porous polymers[12], charged microdroplets,[17,18] microdiameter emulsions,[19] inverted micelles,[20] aerosol particles[21] and porous silica nanoreactor[22,23] etc.

In this contribution, we utilized a porous plasmonic hollow nanoshell as a nanoreactor to run confined chemical reactions. Importantly, this plasmonic nanoreactor offers opportunities to spatially control

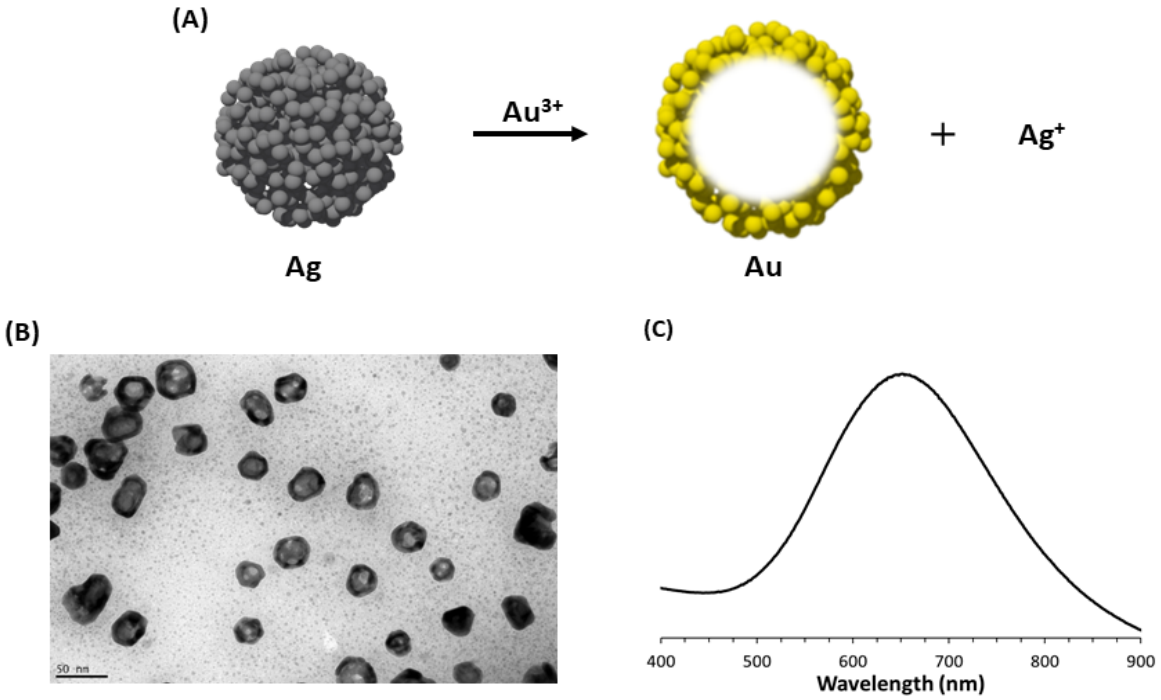

FIGURE 1 (A) Schematic cartoon illustrating the synthesis of AuNS particles. (B) TEM image of as prepared AuNS particles. (C) UV/Vis absorption spectrum of as prepared AuNS particles.

chemical reactions by plasmonic and/or nanoconfinement effects. With the reduction of Ag^+ as a model system, we studied the reaction process systematically with UV-Vis spectroscopy, DLS, Zeta-potential and TEM/STEM elemental mapping. We found that the reduction of Ag^+ preferentially occurred inside the nanoreactor rather than on its external surface. Experiments performed under illumination with white light, at near plasmonic resonance and in the dark suggest that nanoconfinement plays a pivotal role in determining the preferred location of the reduction reaction.

METHODS

Hollow noble metal nanoparticles are of significant interest in fundamental research as well as for chemical/biological applications due to their unique optical properties[24,25] as well as the capability to encapsulate molecular moieties.[26,27] Generally the hollow metal nanoparticles are synthesized by a galvanic replacement reaction, where the salt of metal with higher reduction potential is added to a suspension containing a metal nanoparticle with lower reduction potential. The formation of the AuNS relies on silver nanoparticles (AgNPs) as sacrificial template according to the following reaction, Equation 1.

$$3Ag(s) + AuCl_4^-(aq) \rightarrow Au(s) + 3Ag^+(aq) + 4Cl^-(aq) \quad (1)$$

Specifically, the standard reduction potential of $AuCl^4/Au$ redox pair is 0.99 V vs the standard hydrogen electrode (SHE), while that of Ag^+/Ag is 0.80V vs SHE. The difference in reduction potential causes the Au to be deposited on the AgNP template upon release of Ag^+ into the solution. Details about the nanoparticle synthesis and characterization procedures are provided in the supporting information.

RESULTS AND DISCUSSION

In a typical synthesis, AuNS particles were prepared using the galvanic replacement method developed by Xia *et. al.*[28] The Au^{3+} ions are reduced and a hollow AuNS forms, Figure 1A. A typical TEM image and UV/Vis absorption spectrum of the as synthesized AuNS particles are shown in Figure 1B and 1C, respectively. The hollow interior is clearly visualized in the TEM image as greyish areas surrounded by darker rims. The size of the AuNS particles are 40±10 nm and the absorption peak maximum appears at ~656 nm. The hydrodynamic size of the AuNS particles, as revealed by DLS is ~60 nm, Figure S1. The particles bear a negative surface charge owing to the presence of the citrate ion on the surface. This yields a zeta potential of -30.6 mV at the native pH of the AuNS suspension is 3.8, Figure S1. It is worthwhile pointing out that the hollow particles prepared according to the galvanic replacement protocol, under the reaction conditions described herein, are not pure Au nanoparticles but rather alloy nanoparticles. For example, the EDX analysis in Figure S2 clearly shows that the AuNS particles consist of ~52% Au and ~48% Ag. Although we cannot distinguish between the oxidation states with EDX, we suggest that silver exists in the form of an Ag/Au alloy and/or as Ag^+ ions attached to the shell, most likely at shell imperfections. This observation is in line with previous studies that propose that the shell consists of an Au/Ag bimetallic alloy.[29-31] In this contribution, we merely use the term AuNS just to keep it consistent with the convention in the literature and for the sake of simplicity.

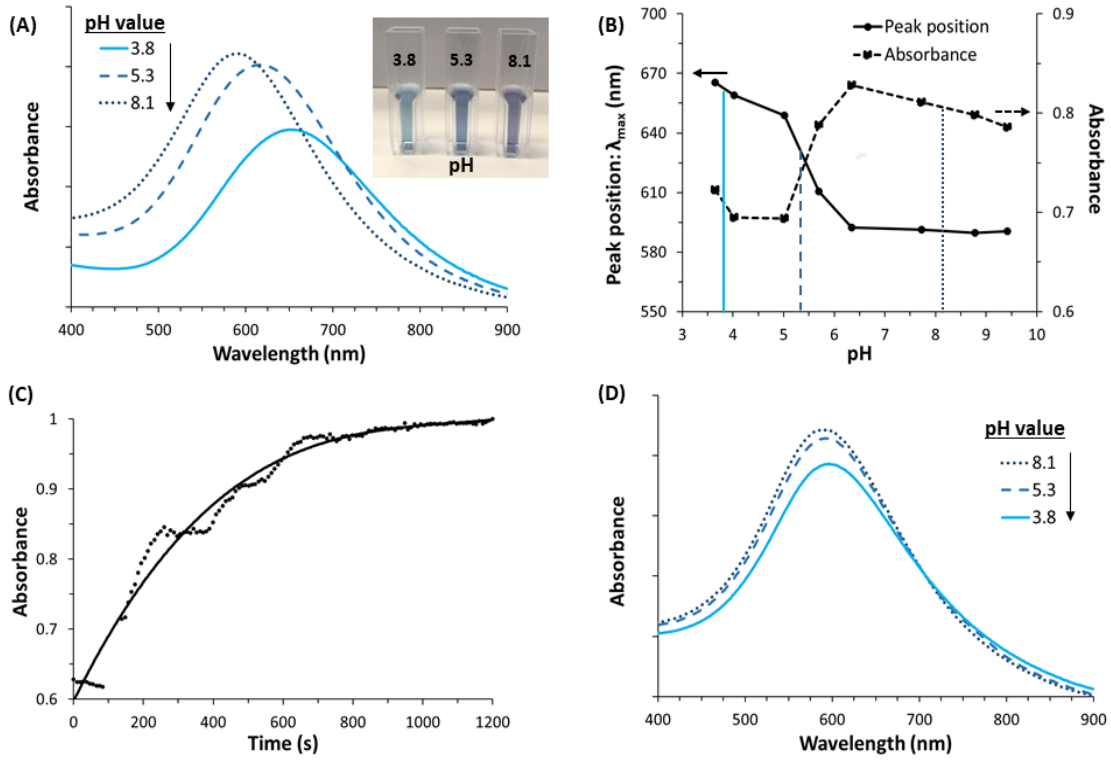

FIGURE 2 (A) Absorbance spectra of AuNS particles in pH 3.8, pH 5.3 and pH 8.1. The pH of the suspension was adjusted with NaOH (0.1 M) from pH 3.8 to pH 8.1. (B) Peak position and absorbance values as a function of pH. (C) Evolution of absorbance at λ_{max} =580 nm with time (black line serves as a guide for the eye). (D) Absorbance spectra of AuNS particles in pH 8.1, pH 5.3 and pH 3.8. The pH of the suspension was adjusted from pH 8.1 to 3.8 upon addition of HNO_3 (0.1 M).

One interesting observation is that the optical spectrum of the AuNS particles is sensitive to changes in the pH of the supporting solution. Figure 2A shows the absorption spectra and photos of AuNS solutions at pH 3.8, 5.3 and 8.1, respectively. The absorption spectrum shifts towards the blue with increasing pH values and the intensity (absorbance) increases. These optical changes are sufficiently large to be visualized by human eye as a blue to purple color transition, see the inset in Figure 2A. The changes in peak maximum and absorbance values of the AuNS suspension with increasing pH is plotted in Figure 2B. It is evident that the blue shift and the concomitant increase in absorbance start at about pH 5 and saturate at pH values above 7.

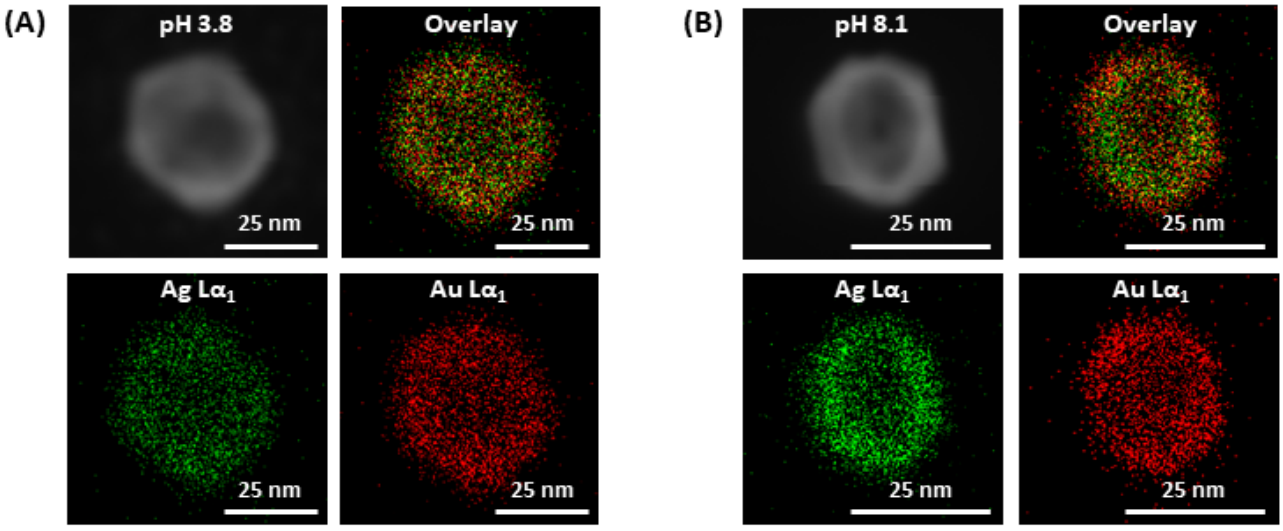

FIGURE 3 STEM elemental mapping (Ag, Au and overlay) of AuNS particles at pH 3.8 (A) and pH 8.1 (B).

Moreover, Figure 2C shows the evolution of the absorbance at 580 nm of a typical AuNS sample with time, when the pH is adjusted to 7 upon addition of NaOH. The kinetics is fast and the reaction saturates within 10 minutes. The kinetics is substantially slower if the reaction start at a lower pH ~5, but it eventually ends up at the same state as that of pH 8, see Figure S3. It is also worthwhile mentioning that this pH-induced transition is not reversible. Thus, when the pH changes back to 3.8, the optical spectrum of AuNS particles does not recover, see Figure 2D and Figure S4. The irreversibility of the optical response suggests that the change is not a simple response to the physical stimulus (change of pH), but rather due to a permanent chemical change in the sample. A possible explanation is that Ag^+ ions are rapidly reduced into Ag and deposited onto the AuNS particles when the pH increases rather than forming individual AgNPs as no peak is seen at ~400 nm. The deposition of Ag on AuNS particles explains the blue shift of the spectrum, as well as the increase in the intensity, because Ag has a higher extinction coefficient and higher resonance frequency (shorter wavelength) than Au.

It is worthwhile to emphasize that the AuNS particles most likely are porous, although they appear as continuous and dense in the TEM images. These pores allow diffusion of

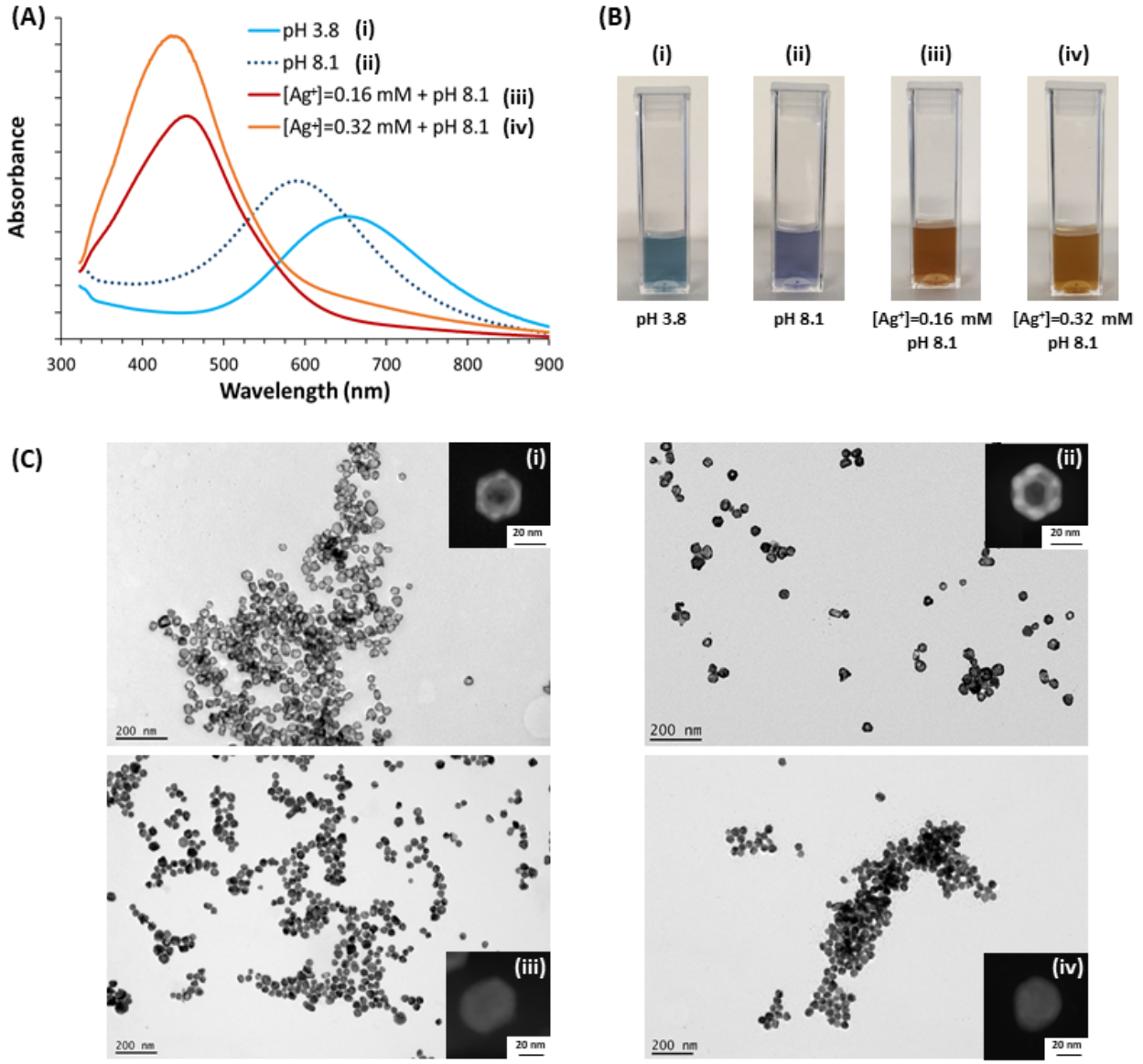

FIGURE 4 (A) Absorbance spectra of AuNS particles in pH 3.8 (blue curve), pH 8.1 (dotted deep blue curve) and addition of silver nitrate before adjusting the pH suspension with NaOH (0.1 M) until pH 8.1: $[Ag^+]$ = 0.16 mM (red curve) and $[Ag^+]$ = 0.32 mM (orange curve). (B) Photos of solutions; and (C) TEM/STEM images of different solutions deposited on TEM grids: (i) pH 3.8; (ii) pH 8.1; (iii) [Ag+] = 0.16 mM, pH 8.1 and (iv) $[Ag^+]$=0.32 mM, pH 8.1, respectively.

reactants (Ag^+, H^+ etc.) and water to and from the interior of the AuNS particles, as evidenced by the fast kinetics shown in Figure 2C. The porous nature of AuNS particles recently was confirmed by other research groups.[29-31] For example, Halas *et. al.* reported that the AuNS particle had small pinholes which allowed for diffusion of Ag^+ ions through pores into the surrounding bath.[31] This group also showed that the dealloying of the nanoshell occurred upon extending the reaction time, eventually resulting in the formation of a pure Au shell particle followed by fragmentation and decomposition. Bedzyk, *et. al.* reported that AuNS particles of similar size and chemical composition consisted of an Au/Ag alloy shell with pores on the atomic scale.[30]

The proposed reduction of Ag^+ and subsequent deposition of Ag onto the AuNS particles for pHs > 5 is supported by previous findings suggesting that the reducing power of sodium citrate increases with pH.[32] Additional characterizations of the AuNS particles at low and high pH values were conducted to investigate the changes, Figure S1. For example, when pH increases from 3.8 to 8.1, the hydrodynamic radius of the AuNS particles decreases from 60.4 nm to 54.4 nm, while the zeta potential changes from -30.6 mV to -39.2 mV. With these and previous observations in mind it seems plausible that Ag^+ ions are reduced and deposited on the AuNS particles thereby leading to distinct changes in their physical/optical properties. An alternative avenue to pH-triggered reduction of Ag^+ ions is to employ a stronger reducing agent than citrate. For example, the same trends in peak shift and absorbance change are seen upon adding 1 mM ascorbic acid to the AuNS suspension, Figure S5.

Transmission and scanning transmission electron microscope (TEM/STEM) experiments were performed to further characterize the particles and to address the growth mechanism of Ag on AuNS particles. Figure 3A shows a TEM image, and the individual Au, Ag and overlay STEM elemental mapping images for the as prepared AuNS particles at pH 3.8. From the individual and overlay elemental images it is clear that elements are distributed uniformly across the nanoparticle. However, for an AuNS sample exposed to pH 8.1, an inhomogeneous distribution of Au and Ag elements is obvious, Figure 3B. In the overlay image, Figure 3B, a green circle (Ag) appears inside the red circle (Au). In addition, the average size of the Ag diameter (green sphere) and Au diameter (red sphere) are measured to equal ~48.1 nm and ~49.5 nm, respectively. These observations suggest that silver reduction preferentially occurs on the inside of the AuNS particles rather than on its external surface. Thus, the inner volume of the AuNS particles appears to work as a nanoreactor, providing spatial control of the reduction reaction and deposition of silver. To further illustrate that the reaction preferentially occurs on the inside of the AuNS particles, we introduced more Ag^+ into the surrounding bath before triggering the reduction by increasing the pH to 8.1.

The extra Ag^+ ions were introduced into the as prepared AuNS suspension and reduced by increasing the pH. Two sets of experiments were conducted by introducing $AgNO_3$ at 0.16 mM and 0.32 mM, respectively. Figure 4A shows the absorption spectra for the two AuNS samples with extra $AgNO_3$ added, as well as for AuNS suspensions without extra $AgNO_3$ for reference purposes. The absorption spectrum is further blue shifted upon addition of Ag^+, and the blue shift increases with the increasing concentration of Ag^+ ions. In particular, for the sample with 0.32 mM $AgNO_3$ added, the resulting spectrum displays a maximum at 435 nm, which is close to the position observed for spherical silver nanoparticles. Figure 4B shows photos of the four sample solutions. It is evident that the addition of Ag induces a color change of the suspension from blue to brown. Large area TEM imaging also was conducted, Figure 4C, see TEM images of the four samples in Figure 4A and B. The vast majority of the AuNS particles appear hollow (low contrast) at low pH and without addition of Ag^+ ions, see image (i), Figure 4C. The AuNS particles become slightly darker upon increasing the pH (ii). Addition Ag^+ ions turn the particles even darker and the AuNS particles appears like solid particles; see the inserts in (iii) and (iv), Figure 4C. Thus, the TEM images clearly demonstrate that the added Ag^+ ions penetrate the shell, become reduced, and fill the empty volume of the AuNS particles until a solid core of Ag is formed.

Further characterization, including zeta potential, DLS size and EDX of the four samples was done; see Figure S1 and Figure S2, and the data are summarized in Table 1. With increasing amount of Ag^+ ions added, the negative zeta potential increases and the size of the resulting nanoparticle increases. Moreover, the absorption peak maximum shifts further towards the blue and the fraction of Ag increases.

Table 1: Summary of physical properties of the four samples prepared at pH 3.8 and pH 8.1, and upon external addition of 0.16 mM and 0.32 mM $AgNO_3$ followed by increasing the pH to 8.1.

Samples	ζ-potential (mV)	DLS (nm)	λ_{max} (nm)	EDX (at. %)
i	-30.6	60.4	656	$Ag_{0.48}Au_{0.52}$
ii	-39.2	54.4	592	$Ag_{0.41}Au_{0.59}$
iii	-49.7	68.9	456	$Ag_{0.75}Au_{0.25}$
iv	-55.1	80.5	435	$Ag_{0.81}Au_{0.19}$

We noticed from the TEM images in Figure 4 that with 0.16 mM $AgNO_3$ (sample iii, Table 1), the initially empty space inside of the AuNS particles appears to be completely filled. From Table 1, however, it is evident that both the size of nanoparticle and the fraction of Ag increase upon increasing the concentration of $AgNO_3$ to 0.32 mM (sample iv, Table 1). Thus, it seems that the reduction of Ag^+ continues after having completely filled the inner volume of the AuNS particles. This phenomenon was carefully investigated using elemental mapping. Figure 5A shows the TEM image, elemental mapping of Au, Ag and the

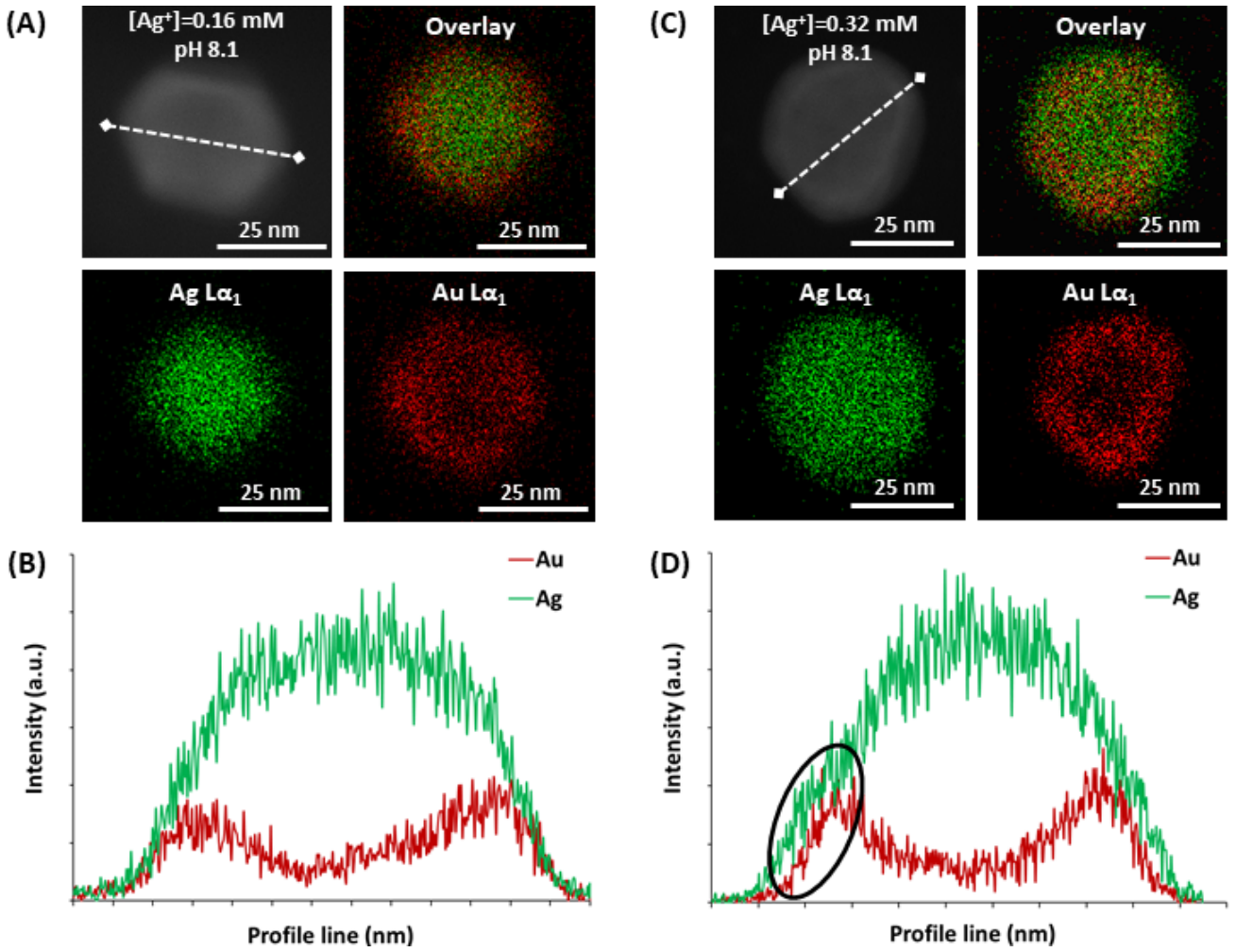

FIGURE 5 TEM and STEM elemental mapping (Ag, Au and overlay) of AuNS particles obtained after adding $AgNO_3$ at pH 3.8 and then increasing the pH to 8.1 for $[Ag^+]$ = 0.16 mM (A) and the corresponding elemental profile along the white hatched line (B). For $[Ag^+]$ = 0.32 mM (C) and the corresponding elemental profile along the white hatched line (D). The black ellipse in (D) highlights the reduction and growth of silver at the external surface once the inner volume is completely filled.

overlay. The profile of Au and Ag along the white hatched line (Figure 5A) is also shown for 0.16 mM $AgNO_3$, Figure 5B. The TEM image reveals a solid nanoparticle and the overlay mapping shows a green core with a shallow red shell structure. The profile of Au and Ag along the white line (Figure 5A) confirms that there is more Ag in the core of the nanoparticle. Figure 5C and D show the TEM image, elemental mapping of Au, Ag and overlay as well as the profile of Au and Ag along the hatched white line after addition of 0.32 mM $AgNO_3$. The TEM image again reveals a solid nanoparticle, and the elemental image is dominated by green color. The size of the green sphere (Ag mapping) is larger than that of the red sphere (Au mapping). Moreover, the line profile of Au and Ag elements in Figure 5D clearly demonstrate the size of Ag is larger than that of Au, as indicated by the black oval circle, see profile plot in Figure 5D. Thus, it appears that the reduction of Ag^+ continues on the external surface when the empty volume inside of AuNS particles is completely filled.

The overall process of Ag^+ reduction and growth on AuNS particles is schematically summarized in Figure 6. The reaction preferentially takes place on the inner walls and proceeds via diffusion through the porous gold nanoshell until the inner volume of the AuNS particles is completely

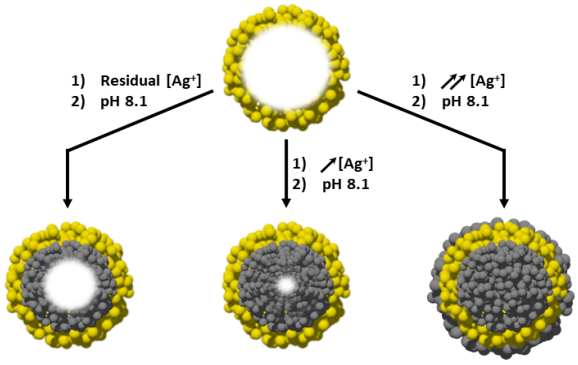

FIGURE 6 Schematic cartoon illustrating the reduction and growth process of silver on the inner and outer surfaces of porous AuNS particles with increasing amounts of silver ions in the surrounding bath.

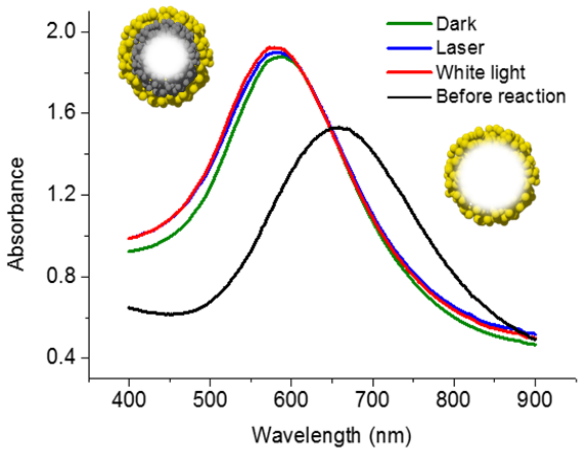

FIGURE 7 Absorption spectra of AuNS particles before initiation of the reaction by increasing the pH (black), and after reaction at pH 8.1 in dark environment (green), under white light illumination (red) and laser illumination (blue), respectively.

filled with silver. The diffusion of ions to the AuNS interior is believed to be driven by concentration gradient or osmotic pressure difference as observed in lipid/polymer vesicle systems.[33] Once the inner volume is completely filled with solid silver the reaction proceeds on the outer surface provided that there is an excess of silver ions in the surrounding bath. The size and properties of the final nanoparticle depend on the reaction conditions, primarily the reaction time and the concentration of silver ions, and it is composed of a solid silver core, a thin layer of gold (the nanoshell) and an outermost silver layer of variable thickness, see Fig 6 (right). It is a compositionally complex nanoparticle whose extinction spectrum resembles that of a spherical AgNP. Thus, the completely filled AuNS particles simply behaves in a similar way as other nanoparticle seeds that initiate deposition of elements at the outside surface.[34,35] The preference of silver reduction inside of AuNS particles is an interesting phenomenon and of significant interest for spatially controlled chemical reactions. In a recent study, Ai *et al.* reported on spatially controlled reduction of Ag^+ at the rim of nanoholes in a periodic Au array.[6] The authors attributed this selective reduction and growth of silver to an electromagnetic field enhancement effect governed by localization of the plasmonic field inside the nanoholes of the array. This phenomenon of localized enhancement of the electric field is well known and has been discussed before for similar plasmonic field-triggered reactions.[36,37] In yet another study on plasmon-mediated reduction of aqueous platinum ions Kim *et al.* proposed an additional effect that contributed to the reduction, namely hot charge carriers.[8]

To further understand the mechanism and the preference of the inner surface of AuNS particles, we investigated the influence of light on the reduction of silver using AuNS particles. Three reactions were performed in parallel at pH 8.1: under white light illumination, at near resonance using a HeNe laser λ=633 nm, and in the dark. Absorption spectra of the resulting nanoparticles are shown in Figure 7. Surprisingly, no significant differences are observed between the three samples. The reaction undoubtedly occurs in the dark, which clearly suggests that the enhanced plasmonic field inside the particle is not the key driving force for the spatially controlled reduction and deposition process. Thus, the well-established explanation of plasmonic field-guided growth and previous observations on other nanostructures[6,9,36] cannot explain the selective growth of silver on the inner walls of AuNS particles. We tentatively propose that it is due to a nanoconfinement effect initiated by reduction of residual silver ions present inside the AuNS particles or in the surrounding bath. Patra *et. al.* also demonstrated that nanoconfinement facilitates the chemical reduction of Ag^+ ion in porous polystyrene beads matrix.[12] It is believed that the nanoconfinement lowers the energy barrier for the electron transfer from reducing agent to Ag^+. Other studies also suggest that the solvents molecules confined in nano space facilitate proton/electron transfer.[15,38]

The interior of AuNS particles provides a perfect space for confined chemical reactions. Moreover, the wall of the AuNS particle is porous which allow reactants to freely diffuse in and out from the inner volume. Another contributing factor to the preferential reduction and deposition of silver on the inner surface might be related to compositional differences between the inner and outer surfaces of the as prepared AuNS particles. It is important to emphasize that the AuNS particles studied herein are prepared by stopping the galvanic replacement reaction after 2 hours. Thus, we end up with bimetallic (alloy) nanoshell particles, see EDX data in Table 1 and supporting information (S2). Complete dealloying of the nanoshell typically requires reaction times >24 hours.[30,31] It is therefore very likely that the inner and outer surfaces are compositionally different and that some elemental silver remains on the inner surface of the nanoshell. This remaining silver can provide favorable sites for reduction and contribute to the preferential reduction and deposition of silver on the inner surface. Besides the Ag^+ reduction demonstrated herein, we believe that the AuNS particles could serve as a general nanosized reactor for confined chemical reactions. Moreover, the understanding of the process of Ag reduction and growth also offers new insights of the complex science and properties of AuNS particles. Interestingly, despite the straightforward synthesis of AuNS particles and decades of widespread applications,[24-26,39] the mechanism behind the AuNS formation is not fully understood.[40] However, Halas *et. al.*[31] and later Bedzyk *et. al.*[30] have contributed substantially to the understanding of the pore formation and de-alloying/fragmentation processes. The study presented herein contributes to the understanding of pH-triggered reduction of silver on the inner walls of AuNS particles that is governed by a continuous supply of Ag^+ ions that diffuses from the external bath into the confined space. Our study also shed light on the subsequent reduction and deposition

occurring on the external surface of the AuNS particles once the inner volume is filled with a solid core of silver.

CONCLUSIONS

We have demonstrated using a suite of experimental techniques that the reduction of sacrificial silver ions present in the surrounding bath preferentially occurs on the inner surface of spherical ~40 nm AuNS particles. The reaction is facilitated by a continuous supply of silver ions that diffuse through the porous AuNS particles into the inner volume where they are rapidly reduced and deposited to form a solid core. We attribute the preferential growth inside the AuNS particles to a nanoconfinement effect rather that of a plasmonic field enhancement effect as the reaction is not influenced by illumination with white light and with a laser beam at near resonance. The findings obtained herein is expected to contribute to a fundamental understanding of spatially controlled reactions at the nanoscale, and potentially also to the development of novel smart nanoscale materials for photonic, catalytic and sensor applications.

ASSOCIATED CONTENT

Supporting Information. Nanoparticle synthesis and characterization procedures. Effect of pH on the size distribution and zeta potential of AuNS particles. EDX measurement of the composition of AuNS. pH-dependent kinetics, and reversibility. Effect of a stronger reducing agent, ascorbic acid. This material is available free of charge via the Internet at http://pubs.acs.org.

AUTHOR INFORMATION

Corresponding Author

Bo Liedberg: bliedberg@ntu.edu.sg, Souhir Boujday souhir.boujday@sorbonne-universite.fr

Author Contributions

The manuscript was written through contributions of all authors. / All authors have given approval to the final version of the manuscript. / ‡These authors contributed equally.

ACKNOWLEDGMENT

We would like to thank the French-Singaporean PHC Merlion program (grant 5.03.15) for financial support. C.P. and B.L. also acknowledge support from the Institute for Nanomedicine jointly established between Northwestern University and Nanyang Technological University. SB, AL, and MS acknowledge the ANR-FWF grant "NanoBioSensor", ANR-15-CE29-0026-02. We would like to dedicate this contribution to Dr. Chen Peng who tragically passed away during the submission stage.

REFERENCES

(1) Assion, A.; Baumert, T.; Bergt, M.; Brixner, T.; Kiefer, B.; Seyfried, V.; Strehle, M.; Gerber, G. Control of chemical reactions by feedback-optimized phase-shaped femtosecond laser pulses. *Science* **1998**, *282*, 919-922.

(2) Wang, L.; Nemoto, Y.; Yamauchi, Y. Direct synthesis of spatially-controlled Pt-on-Pd bimetallic nanodendrites with superior electrocatalytic activity. *J. Am. Chem. Soc.* **2011**, *133*, 9674-9677.

(3) Lv, W.; Lee, K. J.; Li, J.; Park, T.-H.; Hwang, S.; Hart, A. J.; Zhang, F.; Lahann, J. Anisotropic Janus catalysts for spatially controlled chemical reactions. *Small* **2012**, *8*, 3116-3122.

(4) Gu, P.; Zhang, W.; Zhang, G. Plasmonic nanogaps: from fabrications to optical applications. *Adv. Mater. Interfaces* **2018**, *5*, 1800648.

(5) Wang, Z.; Ai, B.; Möhwald, H.; Zhang, G. Colloidal lithography meets plasmonic nanochemistry. *Adv. Opt. Mater.* **2018**, 6, 1800402.

(6) Ai, B.; Wang, Z.; Möhwald, H.; Zhang, G. Plasmonic nanochemistry based on nanohole array. *ACS Nano* **2017**, *11*, 12094-12102.

(7) Maillard, M.; Huang, P.; Brus, L. Silver nanodisk growth by surface plasmon enhanced photoreduction of adsorbed [Ag+]. *Nano Lett.* **2003**, *3*, 1611-1615.

(8) Kim, N. H.; Meinhart, C. D.; Moskovits, M. Plasmon-mediated reduction of aqueous platinum ions: the competing roles of field enhancement and hot charge carriers. *J. Phys. Chem. C.* **2016**, *120*, 6750-6755.

(9) Ueno, K.; Juodkazis, S.; Shibuya, T.; Yokota, Y.; Mizeikis, V.; Sasaki, K.; Misawa, H. Nanoparticle plasmon-assisted two-photon polymerization induced by incoherent excitation source. *J. Am. Chem. Soc.* **2008**, *130*, 6928-6929.

(10) Polak, M.; Rubinovich, L. Nanochemical equilibrium involving a small number of molecules: a prediction of a distinct confinement effect. *Nano Lett.* **2008**, *8*, 3543-3547.

(11) Vaida, V. Prebiotic phosphorylation enabled by microdroplets. *Proc. Nat. Acad. Sci.* **2017**, *114*, 12359-12361.

(12) Patra, S.; Pandey, A. K.; Sen, D.; Ramagiri, S. V.; Bellare, J. R.; Mazumder, S.; Goswami, A. Redox decomposition of silver citrate complex in nanoscale confinement: an unusual mechanism of formation and growth of silver nanoparticles. *Langmuir* **2014**, *30*, 2460-2469.

(13) Patra, S.; Pandey, A. K.; Sarkar, S. K.; Goswami, A. Wonderful nanoconfinement effect on redox reaction equilibrium. *RSC Adv.* **2014**, *4*, 33366-33369.

(14) Rubinovich, L.; Polak, M. The intrinsic role of nanoconfinement in chemical equilibrium: evidence from DNA hybridization. *Nano Lett.* **2013**, *13*, 2247-2251.

(15) Muñoz-Santiburcio, D.; Marx, D. Chemistry in nanoconfined water. *Chem. Sci.* **2017**, *8*, 3444-3452.

(16) Ramaswamy, R.; González-Segredo, N.; Sbalzarini, I. F.; Grima, R. Discreteness-induced concentration inversion in mesoscopic chemical systems. *Nature Commun.* **2012**, *3*, 779.

(17) Banerjee, S.; Gnanamani, E.; Yan, X.; Zare, R. N. Can all bulk-phase reactions be accelerated in microdroplets? *Analyst* **2017**, *142*, 1399-1402.

(18) Yan, X.; Bain, R. M.; Cooks, R. G. Organic reactions in microdroplets: reaction acceleration revealed by mass spectrometry. *Angew. Chem. Inter. Ed.* **2016**, *55*, 12960-12972.

(19) Fallah-Araghi, A.; Meguellati, K.; Baret, J.-C.; El Harrak, A.; Mangeat, T.; Karplus, M.; Ladame, S.; Marques, C. M.; Griffiths, A. D. Enhanced chemical synthesis at soft interfaces: a universal reaction-adsorption mechanism in microcompartments. *Phys. Rev. Lett.* **2014**, *112*, 028301.

(20) Wiebenga-Sanford, B. P.; DiVerdi, J.; Rithner, C. D.; Levinger, N. E. Nanoconfinement's dramatic impact on proton exchange between glucose and water. *J. Phys. Chem. Lett.* **2016**, *7*, 4597-4601.

(21) Griffith, E. C.; Vaida, V. In situ observation of peptide bond formation at the water–air interface. *Proc. Nat. Acad. Sci.* **2012,** 109, 15697-15701.

(22) Koo, J. H.; Kumar, A.; Lee, S.; Jin, X.; Jeong, H.; Kim, J.; Lee, I. S. Pore-engineered silica nanoreactors for chemical interaction-guided confined synthesis of porous platinum nanodendrites. *Chem. Mater.* **2018**, *30*, 3010-3018.

(23) Kim, D.; Choi, J. K.; Kim S. M.; Hwang, I.; Koo, J.; Choi, S.; Cho, S. H.; Kim, K.; Lee, I. S. Confined nucleation and growth of PdO nanocrystals in a seed-free solution inside hollow nanoreactor. *ACS Appl. Mater. Interfaces* **2017**, *9*, 29992-30001.

(24) Sun, Y.; Xia, Y. Increased sensitivity of surface plasmon resonance of gold nanoshells compared to that of gold solid colloids in response to environmental changes. *Anal. Chem.* **2002**, *74*, 5297-5305.

(25) Lu, W.; Melancon, M. P.; Xiong, C.; Huang, Q.; Elliott, A.; Song, S.; Zhang, R.; Flores, L. G.; Gelovani, J. G.; Wang, L. V. et al. Effects of photoacoustic imaging and photothermal ablation therapy mediated by targeted hollow gold nanospheres in an orthotopic mouse xenograft model of glioma. *Cancer Res.* **2011**, *71*, 6116-6121.

(26) You, J.; Zhang, G.; Li, C. Exceptionally high payload of doxorubicin in hollow gold nanospheres for near-infrared light-triggered drug release. *ACS Nano* **2010**, *4*, 1033-1042.

(27) Moon, G. D.; Choi, S.-W.; Cai, X.; Li, W.; Cho, E. C.; Jeong, U.; Wang, L. V.; Xia, Y. A New theranostic system based on gold nanocages and phase-change materials with unique features for photoacoustic imaging and controlled release. *J. Am. Chem. Soc.* **2011**, *133*, 4762-4765.

(28) Sun, Y.; Mayers, B. T.; Xia, Y. Template-engaged replacement reaction: a one-step approach to the large-scale synthesis of metal nanostructures with hollow interiors. *Nano Lett.* **2002**, *2*, 481-485.

(29) Sun, Y.; Xia, Y. Alloying and dealloying processes involved in the preparation of metal nanoshells through a galvanic replacement reaction. *Nano Lett.* **2003**, *3*, 1569-1572.

(30) Moreau, L. M.; Schurman, C. A.; Kewalramani, S.; Shahjamali, M. M.; Mirkin, C. A.; Bedzyk, M. J. How Ag nanospheres are transformed into AgAu nanocages. *J. Am. Chem. Soc.* **2017**, *139*, 12291-12298.

(31) Goodman, A. M.; Cao, Y.; Urban, C.; Neumann, O.; Ayala-Orozco, C.; Knight, M. W.; Joshi, A.; Nordlander, P.; Halas, N. J. The surprising in vivo instability of near-IR-absorbing hollow Au–Ag nanoshells. *ACS Nano* **2014**, *8*, 3222-3231.

(32) Dong, X.; Ji, X.; Wu, H.; Zhao, L.; Li, J.; Yang, W. Shape control of silver nanoparticles by stepwise citrate reduction. *J. Phys. Chem. C* **2009**, *113*, 6573-6576.

(33) Oglęcka, K.; Rangamani, P.; Liedberg, B.; Kraut, R. S.; Parikh, A. N. Oscillatory phase separation in giant lipid vesicles induced by transmembrane osmotic differentials. *Elife* **2014**, *3*, e03695.

(34) Shahjamali, M. M.; Bosman, M.; Cao, S.; Huang, X.; Saadat, S.; Martinsson, E.; Aili, D.; Tay, Y. Y.; Liedberg, B.; Loo, S. C. J. et al. Gold coating of silver nanoprisms. *Adv. Func. Mater.* **2012**, *22*, 849-854.

(35) Rodríguez-Lorenzo, L.; De La Rica, R.; Álvarez-Puebla, R. A.; Liz-Marzán, L. M.; Stevens, M. M. Plasmonic nanosensors with inverse sensitivity by means of enzyme-guided crystal growth. *Nature Mater.* **2012**, *11*, 604-607.

(36) Nguyen, V.-Q.; Ai, Y.; Martin, P.; Lacroix, J.-C. Plasmon-induced nanolocalized reduction of diazonium salts. *ACS Omega* **2017**, *2*, 1947-1955.

(37) Violi, I. L.; Gargiulo, J.; von Bilderling, C.; Cortés, E.; Stefani, F. D. Light-induced polarization-directed growth of optically printed gold nanoparticles. *Nano Lett.* **2016**, *16*, 6529-6533.

(38) Li, S.; Thompson, W. H. Proton transfer in nanoconfined polar solvents. 1. free energies and solute position. *J. Phys. Chem. B* **2005**, *109*, 4941-4946.

(39) Ma, Y.; Liang, X.; Tong, S.; Bao, G.; Ren, Q.; Dai, Z. Gold nanoshell nanomicelles for potential magnetic resonance imaging, light-triggered drug release, and photothermal therapy. *Adv. Func. Mater.* **2013**, *23*, 815-822.

(40) Chee, S. W.; Tan, S. F.; Baraissov, Z.; Bosman, M.; Mirsaidov, U. Direct observation of the nanoscale Kirkendall effect during galvanic replacement reactions. *Nature Commun.* **2017**, *8*, 1224.

TOC Graphic

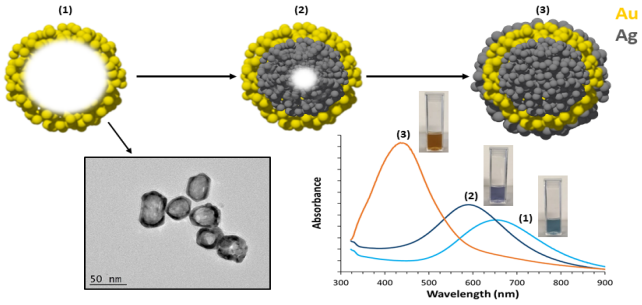
(1)
(2)
(3)
Au
Ag
50 nm
Absorbance
Wavelength (nm)
300
400
500
600
700
800
900